Oncogene (2016), 1–10

www.nature.com/onc

ORIGINAL ARTICLE

Rad54 and Mus81 cooperation promotes DNA damage repair and restrains chromosome missegregation

S El Ghamrasni[1,6], R Cardoso[1,6], L Li[1], KKN Guturi[1], VA Bjerregaard[2], Y Liu[2], S Venkatesan[3], MP Hande[3], JT Henderson[4], O Sanchez[5], ID Hickson[2], A Hakem[1] and R Hakem[1]

Rad54 and Mus81 mammalian proteins physically interact and are important for the homologous recombination DNA repair pathway; however, their functional interactions *in vivo* are poorly defined. Here, we show that combinatorial loss of Rad54 and Mus81 results in hypersensitivity to DNA-damaging agents, defects on both the homologous recombination and non-homologous DNA end joining repair pathways and reduced fertility. We also observed that while Mus81 deficiency diminished the cleavage of common fragile sites, very strikingly, Rad54 loss impaired this cleavage to even a greater extent. The inefficient repair of DNA double-strand breaks (DSBs) in *Rad54*$^{-/-}$*Mus81*$^{-/-}$ cells was accompanied by elevated levels of chromosome missegregation and cell death. Perhaps as a consequence, tumor incidence in *Rad54*$^{-/-}$*Mus81*$^{-/-}$ mice remained comparable to that in *Mus81*$^{-/-}$ mice. Our study highlights the importance of the cooperation between Rad54 and Mus81 for mediating DNA DSB repair and restraining chromosome missegregation.

Oncogene advance online publication, 15 February 2016; doi:10.1038/onc.2016.16

INTRODUCTION

The mammalian genome is constantly exposed to endogenous and exogenous insults including radical oxygen species, DNA replication errors, ionizing radiation (IR) and chemical compounds.[1] DNA double-strand breaks (DSBs) are among the most deleterious DNA alterations. If not repaired properly, these lesions can induce cell death, senescence or promote genomic instability. The repair of DSBs is mediated by either the non-homologous end joining (NHEJ) pathway, which is error-prone producing nucleotide alterations at the sites of rejoining, or through the relatively error-free homologous recombination (HR) pathway initiated by resection of the DSBs and the subsequent invasion of sister chromatids (or homologous chromosomes) by the DNA single strands.[2]

The repair of DSBs is critical for the maintenance of genomic integrity.[1,2] For instance, mutations of genes involved in the HR repair pathway (for example, *Brca1* and *Brca2*) not only increase sensitivity to IR and interstrand cross-linking (ICL) agents (for example, Mitomycin C 'MMC'), but also promote genomic instability.[1] Rad54, a member of the SNF2/SWI2 family, has an important role in the HR repair pathway.[3] Rad54 interacts with Rad51 to promote the assembly and function of the Rad51 nucleoprotein filament and facilitate the strand invasion step required for this repair process.[4] Deficiency of Rad54 in mouse embryonic stem (ES) cells impairs HR-mediated repair and increases sensitivity of these cells to IR and MMC.[5–8] However, although *Rad54*$^{-/-}$ mice also show enhanced sensitivity to MMC, their response to radiation is similar to wild-type (*WT*) mice.[8,9] Consistent with the role of Rad54 in DSB repair, mutations at this locus have been identified in a number of human cancers including non-Hodgkin's lymphoma, colon adenocarcinoma and ductal breast carcinoma.[10,11]

Rad54 physically interacts with Mus81 and stimulates its function.[12] Mus81, together with its partners EME1 or EME2, forms a DNA structure-specific endonuclease important for the restart of stalled replication forks and the resolution of Holliday junctions, which are critical intermediates of HR-mediated repair of DSBs.[13] Mutations of mammalian Mus81 lead to hypersensitivity to ICL agents and increased genomic instability.[14–20] We have also previously reported that *Mus81*$^{\Delta ex3\text{-}4/\Delta ex3\text{-}4}$ (*Mus81*$^{-/-}$) mutant mice display increased predisposition to cancer[14,15,18,20] and down-regulation of Mus81 has been observed in human cancers including hepatocellular carcinoma.[21–23]

Although Rad54 and Mus81 are important for the DNA damage repair in mammalian cells, their functional interactions *in vivo* and the pathological effects of their combined inactivation have not been reported. Here, we investigated the role Rad54 and Mus81 have in the repair of DSBs, genomic integrity and the suppression of tumorigenesis. We report that *Rad54*$^{-/-}$*Mus81*$^{-/-}$ mice and cells are highly sensitive to IR and MMC treatment. Compared with single mutants, *Rad54*$^{-/-}$*Mus81*$^{-/-}$ cells displayed increased frequency of DSBs and more pronounced defects of both HR and NHEJ repair pathways. However, examination of metaphase spreads of *Rad54*$^{-/-}$*Mus81*$^{-/-}$ B cells demonstrated similar levels of chromosomal aberrations compared with the single mutants, and tumor incidence of double mutant mice remained similar to *Mus81*$^{-/-}$ controls. Interestingly, our analyses demonstrate elevated chromosome missegregation and cell death levels in the

[1]Department of Medical Biophysics, University of Toronto and Princess Margaret Cancer Centre, University Health Network, Toronto, Ontario, Canada; [2]Department of Cellular and Molecular Medicine, Center for Chromosome Stability and Center for Healthy Ageing, University of Copenhagen, Panum Institute, Copenhagen, Denmark; [3]Department of Physiology, Yong Loo Lin School of Medicine and Tembusu College, National University of Singapore, Singapore; [4]Department of Pharmaceutical Sciences, Division of Biomolecular Science, Leslie Dan Faculty of Pharmacy, University of Toronto, Toronto, Ontario, Canada and [5]Department of pathology, University of Ontario Institute of Technology, Oshawa, Ontario, Canada. Correspondence: Professor R Hakem, Department of Medical Biophysics, University of Toronto and Princess Margaret Cancer Centre, University Health Network, Toronto, ON M5G 2M9, Canada.
E-mail: rhakem@uhnres.utoronto.ca
[6]These authors contributed equally to this work.
Received 11 August 2015; revised 3 November 2015; accepted 10 November 2015

absence of both Rad54 and Mus81 compared with single mutant controls, suggesting these defects may serve to prevent increased tumor incidence in *Rad54*$^{-/-}$*Mus81*$^{-/-}$ mice compared with *Mus81*$^{-/-}$ littermates.

RESULTS

Combined inactivation of Rad54 and Mus81 does not impair embryonic viability or development of immune cells, but does diminish fertility

To examine the *in vivo* effects of combinatorial loss of Rad54 and Mus81, we generated *Rad54*$^{-/-}$*Mus81*$^{-/-}$ mice by crossing *Rad54*$^{-/-}$ mice[5] to *Mus81*$^{\Delta ex3\text{-}4/\Delta ex3\text{-}4}$ mutant mice.[24] *Rad54*$^{-/-}$*Mus81*$^{-/-}$ mice were obtained at the expected Mendelian ratio and showed no gross developmental defects (Supplementary Table S1). Examination of immune cells in the bone marrow, spleen and thymus from 6- to 8-week-old *Rad54*$^{-/-}$*Mus81*$^{-/-}$ mice showed no difference in total cell numbers compared with their *Rad54*$^{-/-}$, *Mus81*$^{-/-}$ and *WT* littermates (Supplementary Figure 1a). Fluorescence-activated cell sorting analysis of cells from these immune organs indicated a similar distribution of the different immune cell sub-populations in *Rad54*$^{-/-}$*Mus81*$^{-/-}$ mice and their littermate controls (Supplementary Figures 1b–d).

Mutations of a number of genes involved in the signaling or repair of DSBs result in impaired fertility in mouse models and human syndromes (for example, Bloom syndrome).[25–28] We therefore examined litter sizes of *Rad54*$^{-/-}$*Mus81*$^{-/-}$ mice and their single mutant controls. Although interbreeding of *Mus81*$^{-/-}$ mice produced litter sizes similar to that of *WT* mice, smaller litters were obtained from intercrosses of *Rad54*$^{-/-}$ mice (Supplementary Figure 2a; $P < 0.01$). Next, we examined litter sizes produced by crossing *Rad54*$^{-/-}$*Mus81*$^{-/-}$ males and females with *WT* mice and observed no difference compared with litter sizes produced by *WT* mice (Supplementary Figure 2a). Interestingly, interbreeding *Rad54*$^{-/-}$*Mus81*$^{-/-}$ mice produced significantly smaller litters even compared with *Rad54*$^{-/-}$ alone (Supplementary Figure 2a; $P < 0.01$). Examination of testes of *Rad54*$^{-/-}$*Mus81*$^{-/-}$ males, and their single mutant and *WT* littermates indicated no differences in the size of the testes. However, hematoxylin and eosin staining of *Rad54*$^{-/-}$*Mus81*$^{-/-}$ testis sections showed evidence of an arrest of spermatogenesis, with most cells blocked in metaphase resulting in a lack of mature sperms cells, (Supplementary Figures 2e–g). In addition, the testes showed severe focal atrophy of the seminiferous tubules, with absence of spermatogenic cells and degenerative vacuolization of Sertoli cells (Supplementary Figure 2h).

Collectively, these data indicate that while combined loss of Rad54 and Mus81 does not affect viability of mouse embryos or homeostasis of the immune system, it leads to defective fertility.

Combinatorial loss of Rad54 and Mus81 leads to *in vivo* and *in vitro* hypersensitivity to ICL agents and IR

Mus81 deficiency has been associated with increased sensitivity to DNA-damaging agents.[14,16,17,29,30] Although Mus81 deficiency in mammalian cells results in hypersensitivity to MMC, it does not affect sensitivity to IR.[14] In contrast, previous studies indicated increased sensitivity of *Rad54*$^{-/-}$ ES cells to both IR and MMC.[5,7] Curiously, however, *Rad54*$^{-/-}$ mice, while highly sensitive to MMC, display similar sensitivity to IR compared with *WT* controls.[8,9] *Mus81*$^{-/-}$ and *Rad54*$^{-/-}$*Mus81*$^{-/-}$ ES cells exhibit similar levels of hypersensitivity to MMC, suggesting the involvement of Rad54 and Mus81 in the same repair pathway of ICL-induced DNA damage in ES cells.[31]

To examine the relationship of Rad54 and Mus81 in the sensitivity to ICLs at the organismal level, we injected cohorts of *Rad54*$^{-/-}$*Mus81*$^{-/-}$, *Rad54*$^{-/-}$, *Mus81*$^{-/-}$ and *WT* mice with MMC (10 mg/kg of body mass) and monitored the survival of these cohorts for 25 days. Although *Rad54*$^{-/-}$ mice exhibited enhanced sensitivity to MMC treatment compared with *WT* controls (Figure 1a; $P < 0.05$), MMC sensitivity was even greater for *Mus81*$^{-/-}$ mice compared with *Rad54*$^{-/-}$ mice (Figure 1a; $P < 0.001$). Interestingly, the MMC sensitivity of *Rad54*$^{-/-}$*Mus81*$^{-/-}$ mice was further increased compared with *Mus81*$^{-/-}$ littermates (Figure 1a; $P < 0.05$).

We next generated SV40-immortalized *Rad54*$^{-/-}$*Mus81*$^{-/-}$ mouse embryonic fibroblast (MEFs) and their single mutants and *WT* controls and examined their sensitivity to MMC using

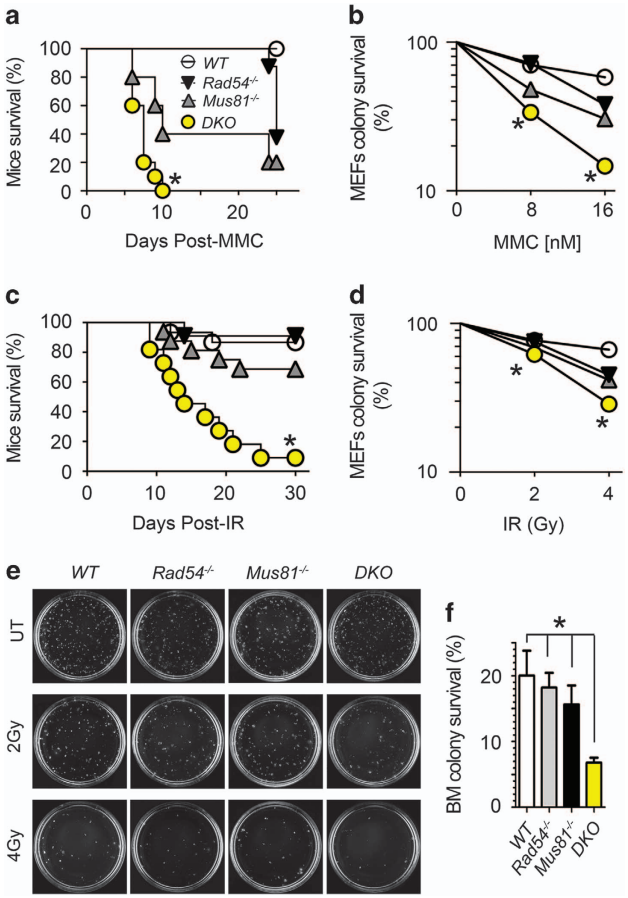

Figure 1. Combinatorial loss of Rad54 and Mus81 leads to hypersensitivity to ICL agents and IR. (**a**) Kaplan–Meier survival analysis of cohorts of age-matched *WT* ($n = 7$), *Rad54*$^{-/-}$ ($n = 7$), *Mus81*$^{-/-}$ ($n = 7$) and *Rad54*$^{-/-}$*Mus81*$^{-/-}$ (DKO; $n = 10$) mice injected with 10 mg MMC/kg of body mass. Mice were monitored for survival for 25 days post-MMC injection. *$P < 0.05$; DKO compared with single mutant controls. (**b**) Graph showing percent survival in a clonogenic assay of SV40-immortalized MEFs treated with MMC. Data are presented as the mean ± s.d. of three independent experiments. *$P < 0.05$; DKO compared with single mutant controls. (**c**) Kaplan–Meier survival analysis of cohorts of age-matched *WT* ($n = 13$), *Rad54*$^{-/-}$ ($n = 11$), *Mus81*$^{-/-}$ ($n = 16$) and DKO ($n = 11$) mice subjected to whole-body IR (8 Gy). Mice were monitored for survival for 30 days post-treatment. *$P < 0.001$; DKO compared with single mutant controls. (**d**) Graph showing percent survival in a clonogenic assay of SV40-immortalized MEFs irradiated with 2 or 4 Gy IR. Data are presented as the mean ± s.d. of three independent experiments. *$P < 0.05$; DKO compared with single mutant controls. (**e**, **f**) Colony-forming assay of bone marrow cells from *Mus81*$^{-/-}$*Rad54*$^{-/-}$ mice and their *Mus81*$^{-/-}$, *Rad54*$^{-/-}$, and *WT* littermate controls. (**e**) Representative pictures of plates showing colonies at day 10 under untreated conditions or post-IR with 2 or 4 Gy. (**f**) Data for 4 Gy IR of bone marrow cells were normalized to untreated cells and are presented as the mean ± s.d. of three independent experiments. *$P < 0.05$; DKO compared with single mutant controls. All statistical analysis was performed using a two-tailed Student's *t*-test.

clonogenic assays. Although *Mus81*$^{-/-}$ MEFs displayed increased sensitivity to both doses of MMC compared with *WT* (Figure 1b; $P < 0.0001$), *Rad54*$^{-/-}$ MEFs were significantly more sensitive compared with *WT* only to a high dose of MMC (Figure 1b; $P < 0.001$). Similarly to the effects seen in *Rad54*$^{-/-}$*Mus81*$^{-/-}$ mice, double mutant MEFs were also significantly more sensitive to MMC compared with single mutants (Figure 1b; $P < 0.001$).

To examine the effect of deficiency of Rad54 and Mus81 on *in vivo* radiosensitivity, *Rad54*$^{-/-}$*Mus81*$^{-/-}$ mice, single mutants and *WT* controls were subjected to 8 Gy of IR and their survival was monitored for a period of 30 days. Although *Rad54*$^{-/-}$ and *Mus81*$^{-/-}$ mice showed no increased radiosensitivity compared with *WT* controls, *Rad54*$^{-/-}$*Mus81*$^{-/-}$ mice were highly radiosensitive with over 90% of the irradiated mice dying before the end of the monitoring period (Figure 1c; $P < 0.001$ compared with *Mus81*$^{-/-}$ mice). Next, we performed clonogenic assays examining the response of SV40-immortalized *Rad54*$^{-/-}$*Mus81*$^{-/-}$ MEFs and their single mutant counterparts and *WT* controls to IR. Although *Rad54*$^{-/-}$ and *Mus81*$^{-/-}$ MEFs showed no significant difference in response to 2 Gy compared with *WT* controls, they exhibited greater sensitivity at 4 Gy (Figure 1d; $P < 0.001$). However, double mutant MEFs showed increased radiosensitivity to both 2 and 4 Gy compared with *WT* controls (Figure 1d; $P < 0.001$), and were more sensitive compared with *Rad54*$^{-/-}$ or *Mus81*$^{-/-}$ MEFs at 4 Gy (Figure 1d; $P < 0.001$).

We also examined the effect of the dual loss of Rad54 and Mus81 on the response of bone marrow cells to IR. Data from clonogenic assays indicated increased radiosensitivity of *Rad54*$^{-/-}$*Mus81*$^{-/-}$ bone marrow cells compared with single mutants and *WT* controls (Figures 1e and f and Supplementary Figure 3a; $P < 0.05$). Similarly, analysis of Annexin V/propidium iodide staining of thymocytes 24 h post 2 Gy of IR indicated increased radiosensitivity of *Rad54*$^{-/-}$*Mus81*$^{-/-}$ thymocytes compared with single mutants and *WT* controls (Supplementary Figure 3b; $P < 0.05$).

Collectively, these data underscore the importance of the cooperation of Rad54 and Mus81 *in vivo* and *in vitro* for the response to DNA damage induced by ICL and IR.

Rad54 and Mus81 cooperate to mediate efficient repair of DSBs

Given that spontaneous genomic instability is elevated in mice and human cells deficient for Mus81 or Rad54,[14–18,20,32] and *Rad54*$^{-/-}$*Mus81*$^{-/-}$ mice and cells exhibit elevated sensitivity to MMC and IR, we examined the effect of combinatorial loss of Rad54 and Mus81 on chromosomal instability. We first examined levels of chromosomal aberrations in metaphase spreads of lipopolysaccharide-activated B cells from *Rad54*$^{-/-}$*Mus81*$^{-/-}$ mice and their single mutants and *WT* littermates. *Rad54*$^{-/-}$ and *Mus81*$^{-/-}$ B cells displayed elevated levels of spontaneous and IR-induced chromosomal aberrations compared with *WT* controls (Figure 2a and Table 1). Examination of metaphases from *Rad54*$^{-/-}$*Mus81*$^{-/-}$ B cells indicated that the levels of spontaneous, as well as MMC- and IR-induced chromosomal aberrations, were similar to those of the single mutant controls (Figure 2a and Table 1).

SV40-immortalized MEFs possess inactivated p53 and Rb pathways and as such display increased resistance to DNA damage.[26,33] We therefore examined levels of spontaneous and IR-induced DSBs in SV40-immortalized *Rad54*$^{-/-}$*Mus81*$^{-/-}$ MEFs and their controls. Levels of γH2ax foci, a marker for DNA breaks,[1] were examined in MEFs either untreated or at different time points post-IR. Under untreated conditions, *Rad54*$^{-/-}$ and *Mus81*$^{-/-}$ MEFs showed increased level of γH2ax foci compared with *WT* MEFs (Figures 2b and c; $P < 0.01$). However, the level of spontaneous DSBs was even greater in double mutant cells compared with single mutants (Figures 2b and c; $P < 0.01$). The retention of γH2ax foci 24 h post-IR was also higher in double mutant MEFs compared with single mutant controls (Figures 2b and c; $P < 0.05$). In accordance with these data, the frequency of 53bp1 foci, another marker of DSBs, was elevated in *Rad54*$^{-/-}$*Mus81*$^{-/-}$ MEFs compared with single mutants, both under untreated conditions and 24 h post-IR (Figures 2d and e; $P < 0.01$). Taken together, these results show a collaboration of Rad54 and Mus81 in DSB repair and the maintenance of genomic integrity.

Rad54 and Mus81 are required for HR- and NHEJ-mediated DSB repair

Mammalian Rad54 and Mus81 have important roles in the HR-mediated repair of DSBs.[4,13] Mus81 is a component of a resolvase that processes Holliday junctions, intermediate structures that arise during HR-mediated repair.[13] In addition to the importance of Rad54 in facilitating the assembly and the function of the Rad51 nucleoprotein filament, a critical step for HR-mediated DSB repair, Rad54 also promotes branch migration of Holliday junctions, Rad54 deficiency in ES cells has also been reported to delay early recruitment of Rad51 to DSB sites.[3,4,34] To examine the effects of loss of mammalian Rad54 and Mus81 on HR-mediated repair of DSBs, we first examined Rad51 recruitment to DSB flanking sites in SV40-immortalized *Rad54*$^{-/-}$*Mus81*$^{-/-}$ and control MEFs. Although at 6 h post-IR, *Rad54*$^{-/-}$ and *Mus81*$^{-/-}$ MEFs displayed a similar level of Rad51 foci compared with *WT* MEFs, the number of these foci was significantly reduced in double mutant MEFs (Figures 3a and b; $P < 0.001$). This raised the possibility that these double mutant cells may have defective HR repair pathway. As HR defects lead to hypersensitivity to poly ADP-ribose polymerase (PARP) inhibitors (PARPis),[35] we performed clonogenic assays using SV40-immortalized MEFs and examined the effects of loss of Rad54 and/or Mus81 loss on PARPi-induced killing. Although *Rad54*$^{-/-}$ and *Mus81*$^{-/-}$ MEFs demonstrated increased sensitivity to PARPi compared with *WT* controls (Figure 3c; $P < 0.01$), the sensitivity of *Rad54*$^{-/-}$*Mus81*$^{-/-}$ MEFs to PARPi was even higher compared with single mutant controls (Figure 3c; $P < 0.01$).

We next used a reporter assay[36] to directly examine the efficiency of HR-mediated repair of DSBs in SV40-immortalized *Rad54*$^{-/-}$*Mus81*$^{-/-}$ MEFs and their single mutants and *WT* controls. Both *Rad54*$^{-/-}$ and *Mus81*$^{-/-}$ MEFs displayed reduced efficiency in HR-mediated repair compared with *WT* controls (Figure 3d; $P < 0.05$). Interestingly, consistent with their more pronounced defect in Rad51 recruitment to DSB sites, and their elevated sensitivity to PARPi, *Rad54*$^{-/-}$*Mus81*$^{-/-}$ MEFs displayed less efficient HR-mediated repair compared with single mutants (Figure 3d; $P < 0.05$).

Some interplay exists between the HR and NHEJ repair pathways, and activation of the NHEJ pathway can compensate for defective HR-mediated repair.[2] Thus, using a reporter assay,[36] we examined the level of NHEJ-mediated repair of DSBs in SV40-immortalized *MEFs* lacking Rad54, Mus81 or both proteins. We observed reduced NHEJ repair in *Rad54*$^{-/-}$ and *Mus81*$^{-/-}$ MEFs compared with *WT* controls (Figure 3e; $P < 0.05$) and unexpectedly this defect was further exacerbated in *Rad54*$^{-/-}$*Mus81*$^{-/-}$ MEFs compared with single mutants (Figure 3e; $P < 0.001$). Next we examined the level of expression of proteins important for HR (Brca1 and Rad51) and NHEJ (53bp1) repair pathways in MEFs from the different genotypes. Consistent with defective HR and NHEJ repair in DKO MEFs, western blot analysis indicated that dual loss of Rad54 and Mus81 decreases level of Brca1, 53bp1 and Rad51 protein expression (Figure 3f). Collectively, these data indicate that combined loss of Rad54 and Mus81 not only impairs the HR repair pathway, it also restrains the efficiency of the NHEJ repair pathway.

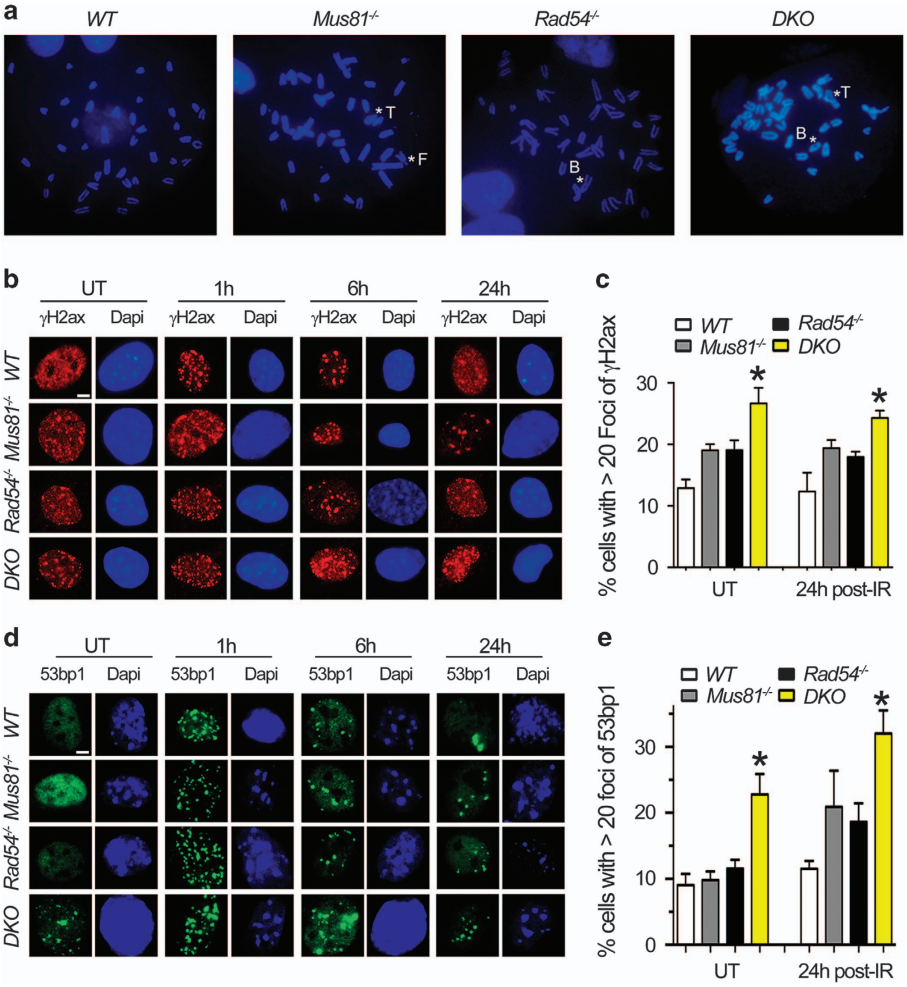

Figure 2. Chromosomal aberrations and increased frequency of spontaneous and unrepaired DSBs in *Rad54*$^{-/-}$*Mus81*$^{-/-}$ cells. (**a**) Representative metaphase spreads of irradiated (2 Gy) lipopolysaccharide (LPS)-activated B cells from *WT*, *Rad54*$^{-/-}$, *Mus81*$^{-/-}$ and *Rad54*$^{-/-}$*Mus81*$^{-/-}$ mice. *Abnormal chromosome. T, triradial; F, fragment; B, break. (**b**) γ-H2ax staining of SV40-immortalized *Rad54*$^{-/-}$ *Mus81*$^{-/-}$MEFs and controls. MEFs were either left untreated (UT) or irradiated (5 Gy) and allowed to recover for 1, 6 and 24 h. Cells were fixed, stained with anti-γ-H2ax antibody and counterstained with DAPI. Scale bars: 2 μm. (**c**) Graphs displaying percentage of cells with >20 foci of γ-H2ax foci under UT or radiation-treated conditions. Data are presented as the means s.d. of at least three independent experiments. At least 100 cells were quantified per experiment. *Denotes statistical significance compared with single mutant controls ($P < 0.05$). (**d**) SV40-immortalized *Rad54*$^{-/-}$*Mus81*$^{-/-}$ MEFs and controls were stained with anti-53bp1 antibody and counterstained with DAPI. (**e**) Graphs displaying percentage of cells with >20 foci for 53bp1. Data are presented as the means s.d. of at least three independent experiments. At least 100 cells were quantified per experiment. *Denotes statistical significance compared with single mutant controls ($P < 0.05$). All statistical analysis was performed using a two-tailed Student's *t*-test.

Rad54$^{-/-}$Mus81$^{-/-}$ mice and Mus81$^{-/-}$ mice display similar risk of tumorigenesis

Defects in the HR and NHEJ repair pathways can promote the development of human cancers.[1] Therefore, we monitored cohorts of *Rad54*$^{-/-}$*Mus81*$^{-/-}$, *Rad54*$^{-/-}$, *Mus81*$^{-/-}$ and *WT* littermate mice for a period of 20 months. Although *Rad54*$^{-/-}$ mice displayed no reduced survival compared with *WT* controls, *Mus81*$^{-/-}$ mice, as previously reported,[14,15,18,20] exhibited a shorter life span because of an increased incidence of tumors (Figure 4a; $P < 0.05$ compared with *WT* controls). However, survival of *Rad54*$^{-/-}$*Mus81*$^{-/-}$ mice remained similar to *Mus81*$^{-/-}$ mice (Figure 4a).

Tumors observed in the *Rad54*$^{-/-}$*Mus81*$^{-/-}$ and *Mus81*$^{-/-}$ cohort of mice were examined by hematoxylin and eosin staining and immunohistochemistry, and the majority of these tumors were B-cell lymphomas (B220^{+}) (Figures 4b–g). These data indicate that despite the higher DSB repair defects in *Rad54*$^{-/-}$*Mus81*$^{-/-}$ mice compared with *Mus81*$^{-/-}$ mutants, tumor predisposition of double mutant mice remains similar to that of *Mus81*$^{-/-}$ littermates.

Deficiency of Rad54 and Mus81 leads to defective chromosomal segregation and increased cell death

The structure-specific endonuclease Mus81-Eme1 localizes to common fragile sites (CFSs) and mediates their cleavage, allowing sister chromatid disjunction.[37,38] Moreover, knockdown of human Mus81 has been shown to induce chromosomal segregation defects.[37–40] Given the presence of CFS on all human chromosomes, and its association with human diseases including cancer,[41,42] we examined whether Rad54 affects these Mus81-dependent functions. Chromatin bridges and cells with micronuclei or multinuclei are features of cells with mitotic defects.[13] Therefore, we examined SV40-immortalized *Rad54*$^{-/-}$ *Mus81*$^{-/-}$MEFs and their controls for the frequency of

Table 1. Effects of dual loss of Rad54 and Mus81 on genomic stability

Sample ID	*Metaphase scored*	*Aberrant cells*	*Fragments/breaks*	*Fusions*	*Triradial-like structures*	*Total aberrations*
WT UT	280	4	4	0	0	4
		1.43	1.43	0.00	0.00	1.43
WT IR	120	5	2	3	0	5
		4.17	1.67	2.50	0.00	4.17
WT MMC	120	10	5	2	5	12
		8.33	4.17	1.67	4.1	10.00
Mus81$^{-/-}$ UT	280	17	12	5	0	17
		6.07	4.29	1.79	0.00	6.07
Mus81$^{-/-}$ IR	120	19	14	9	0	23
		15.83	11.67	7.50	0.00	19.17
Mus81$^{-/-}$ MMC	108	38	21	15	10	46
		31.67	17.50	12.50	8.33	38.33
Rad54$^{-/-}$ UT	200	17	6	6	1	13
		7.00	3.00	3.00	0.50	6.50
Rad54$^{-/-}$ IR	120	23	11	11	2	25
		19.17	9.17	9.17	2.50	20.83
Rad54$^{-/-}$ MMC	160	46	28	26	9	63
		28.75	17.50	16.25	5.63	39.38
DKO UT	200	11	4	7	2	13
		5.50	2.00	3.50	1.00	6.50
DKO IR	120	28	15	14	4	33
		23.33	12.50	11.67	3.33	27.50
DKO MMC	160	57	24	32	15	71
		35.63	15.00	20.00	9.38	44.38

Abbreviations: IR, ionizing radiation; LPS, lipopolysaccharide; MMC, Mitomycin C; UT, untreated; WT, wild type. Metaphase spreads of LPS-activated B cells were examined for spontaneous, MMC or IR-induced chromosomal aberrations. $P = 0.006$; UT *WT* vs UT *Mus81*$^{-/-}$. $P = 1.949^{e-10}$; UT *WT* vs UT *DKO*. $P = 0.0006$; 2 Gy *WT* vs 2 Gy *Mus81*$^{-/-}$ or 2 Gy *Rad54*$^{-/-}$. $P = 6.425^{e-7}$; 2 Gy *WT* vs 2 Gy *DKO*. $P = 1.758^{e-8}$; MMC *WT* vs MMC *Mus81*$^{-/-}$ or MMC *Rad54*$^{-/-}$. $P = 1.949^{e-10}$; MMC *WT* vs MMC *DKO*. Two-sided Fisher's exact test using the Mstat software was used for comparison of the frequency of chromosomal aberrations. Second row—percentage data shown. Fusions involve dicentrics, sister chromatid fusion, ring chromosomes and Robertsonian fusion-like configurations. Triradial-like structures include quadriradials and multicentric chromosomes.

multinucleated cells and cells that display micronuclei or the presence of chromatin bridges. Although the frequency of cells with these aberrations was similar between single mutants and *WT* MEFs, we observed higher number of *Rad54*$^{-/-}$*Mus81*$^{-/-}$ mutant MEFs with multinuclei, micronuclei or chromatin bridges (Figures 5a–f). Taken together, these results suggest that dual loss of Rad54 and Mus81 impairs mitotic chromosome segregation.

Mus81 mediates fragile site breakage in human cells.[37,38] In order to evaluate the potential role of Mus81 and/or Rad54 in this process in mouse cells, we quantified the frequency of metaphase chromosome fragility in B cells treated with low dose of aphidicolin (Table 2 and Supplementary Figure 4). As expected, B cells from *WT* mice showed a significant increase in fragile site breakage following aphidicolin treatment (2.5-fold; $P = 1.91e^{-5}$). Similarly, and as seen previously in human cells, Mus81 deficiency led to an attenuation of this increase (increase of only 1.4-fold; $P = 0.09$). Interestingly, however, both *Rad54*$^{-/-}$ and *Rad54*$^{-/-}$ *Mus81*$^{-/-}$ B cells showed either little or no aphidicolin-induced breakage ($P = 0.5$). These results indicate a conservation of a role for Mus81 in the generation of replicative stress-inducible fragile site breakage, but reveal an unexpected and major role for Rad54 in this process. These results also suggest that components of the HR pathway have a hitherto poorly defined role in the creation of chromosome fragility.

Despite an increase in chromosomal missegregation and impaired DSB repair of *Rad54*$^{-/-}$*Mus81*$^{-/-}$ cells, the double mutant mice displayed no increased incidence of tumors compared with their *Mus81*$^{-/-}$ littermates. We therefore examined whether cell death, a mechanism that protects cells from malignant transformation, may be elevated in *Rad54*$^{-/-}$*Mus81*$^{-/-}$ mice. Terminal deoxynucleotidyl transferase-mediated dUTP nick end labeling (TUNEL) staining of splenocytes from *Rad54*$^{-/-}$*Mus81*$^{-/-}$ mice and their single mutant and *WT* littermates indicated elevated levels of cell death (TUNEL-positive cells) in spleen sections of *Rad54*$^{-/-}$ *Mus81*$^{-/-}$ mice compared with single mutant and *WT* littermates (Figure 5g). In addition, cell number of splenocytes from 12 to 13 months old *Rad54*$^{-/-}$*Mus81*$^{-/-}$, *Rad54*$^{-/-}$, *Mus81*$^{-/-}$ and *WT* littermate mice showed significantly reduced ($P < 0.001$) number of splenocytes in *DKO* mice ($46.3 \times 10^6 \pm 2.603$) compared with *Mus81*$^{-/-}$ ($79.67 \times 10^6 \pm 2.333$) *Rad54*$^{-/-}$ ($72 \times 10^6 \pm 1.732$) and *WT* ($80.67 \times 10^6 \pm 2.839$) controls (Figure 5h). Collectively, these results indicate that combinatorial loss of Rad54 and Mus81 leads to mitotic defects, decreased breakage at CFS and elevated cell death levels.

DISCUSSION

Rad54 and Mus81 are important components of the HR-mediated pathway for repair of DSBs in mammalian cells[13,43] and defects in either of these factors sensitize cells to DNA-damaging agents and promote genomic instability.[3,6,14,31] However, whether dual loss of Rad54 and Mus81 would lead to similar or more pronounced defects of the repair of DSBs has not been addressed previously.

In this study, we report that dual loss of Rad54 and Mus81 does not affect embryonic development. However, interestingly, our data have uncovered a cooperative effect of mammalian Rad54 and Mus81 on fertility, as *Rad54*$^{-/-}$*Mus81*$^{-/-}$ males display testicular defects and intercrossing of *Rad54*$^{-/-}$*Mus81*$^{-/-}$ mice produces smaller litters compared with single mutant controls. Previous studies indicated hypersensitivity of human and mouse cells deficient for Rad54 or Mus81 to MMC,[5,6,14,31,44] and studies in ES cells have suggested an epistatic relationship between Rad54 and Mus81 in response to MMC.[31] By contrast, we observed higher MMC and IR sensitivity levels for *Rad54*$^{-/-}$*Mus81*$^{-/-}$ mice, bone marrow cells, thymocytes and MEFs compared with single mutants. Thus, defects in Rad54 and Mus81 have synergistic

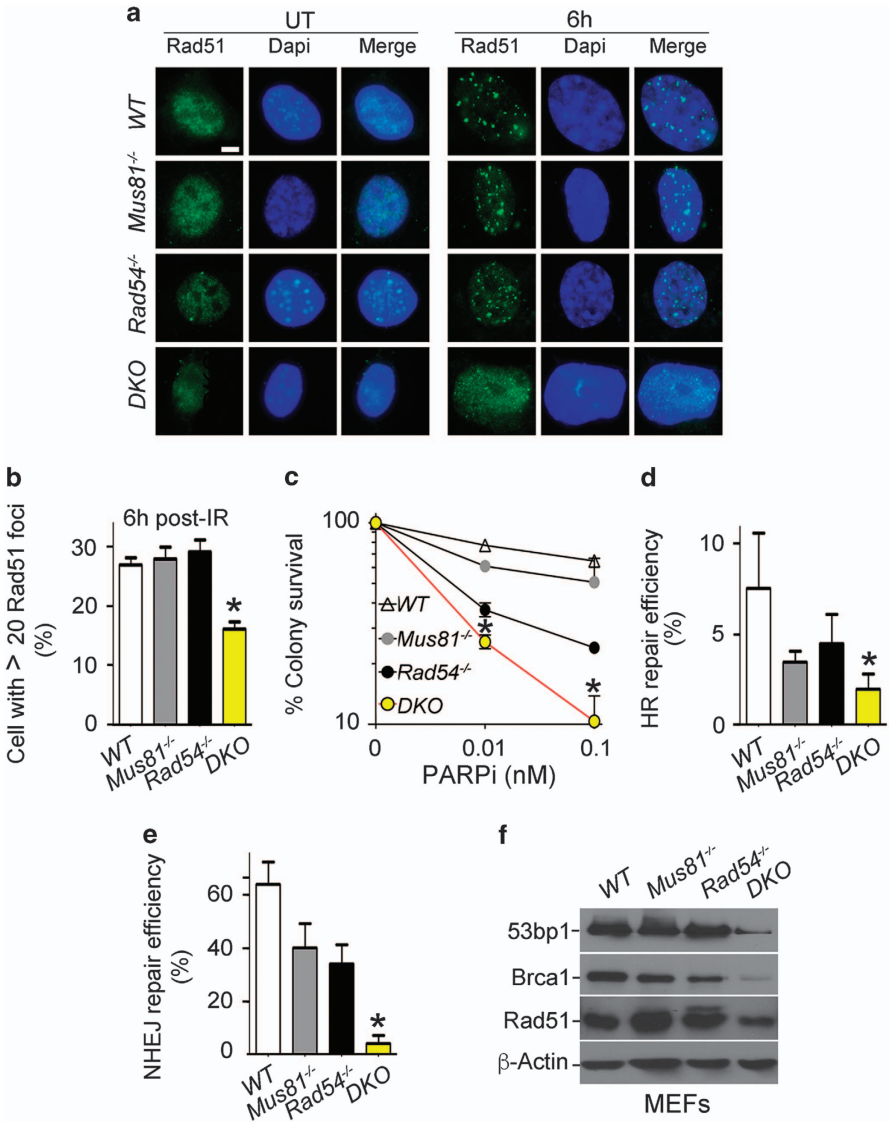

Figure 3. Dual loss of Rad54 and Mus81 impairs HR and NHEJ repair pathways. (**a**) Rad51 staining of SV40-immortalized DKO MEFs and controls. MEFs were either left untreated (UT) or irradiated (5 Gy), allowed to recover for 6 h, and then stained using an anti-Rad51 antibody and counterstained with DAPI. (**b**) Percentage of cells showing >20 Rad51 foci 6 h post-irradiation. Data are presented as the means s.d. of at least three independent experiments. At least 100 cells were quantified per experiment. *Denotes statistical significance compared with single mutant controls ($P < 0.05$). (**c**) Graph showing survival percentage in a clonogenic assay, of SV40-immortalized MEFs treated with PARPi. Data are presented as the mean ± s.d. of three independent experiments. *$P < 0.05$; DKO cells compared with single mutant controls. (**d**) Graphs showing the percentage of HR repair efficiency of SV40-immortalized *Rad54*$^{-/-}$*Mus81*$^{-/-}$, *Rad54*$^{-/-}$, *Mus81*$^{-/-}$ and *WT* MEFs. MEFs were co-transfected with the linearized pHR reporter and undigested RFP plasmid, and fluorescence-activated cell sorting (FACS) analysis was performed 48 h post-transfection. *Denotes statistical significance of DKO cells compared with single mutant controls ($n = 5$; $P < 0.01$). (**e**) Graphs showing the percentage of NHEJ repair efficiency of SV40-immortalized *Rad54*$^{-/-}$*Mus81*$^{-/-}$, *Rad54*$^{-/-}$, *Mus81*$^{-/-}$ and *WT* MEFs. MEFs were co-transfected with the linearized pNHEJ reporter and undigested RFP plasmid and FACS analysis was performed 48 h post-transfection. *Denotes statistical significance of DKO cells compared with single mutant controls ($n = 5$; $P < 0.001$). (**f**) Representative western blot analysis of 53bp1, Brca1 and Rad51 expression in untreated SV40-immortalized MEFs. All statistical analysis was performed using a two-tailed Student's *t*-test.

effects not only on fertility, but also on the response to ICL agents and IR; although, this could be dependent upon the cellular context and type.

Based on previous studies showing that lack of either Rad54 or Mus81 promotes genomic instability, we expected that combinatorial loss of these two proteins would further impair chromosomal stability. However, analysis of metaphase spreads of *Rad54*$^{-/-}$*Mus81*$^{-/-}$ B cells failed to show increased levels of chromosomal aberrations compared with single mutants. Although this could results from a lack of synergistic effects of the two mutations in B cells, it could also be due to elevated levels of apoptosis of the B cells in response to DNA damage. Indeed, our analysis of SV40-immortalized MEFs, which are resistant to apoptosis, indicates increased levels of spontaneous DSBs and unrepaired breaks following IR in *Rad54*$^{-/-}$*Mus81*$^{-/-}$ MEFs compared with single mutant controls.

The increased incidence of unrepaired DSBs in *Rad54*$^{-/-}$*Mus81*$^{-/-}$ MEFs also correlates with their inability to recruit Rad51 to DSB flanking sites and their elevated defects of HR-mediated repair compared with single mutants. Remarkably, the NHEJ pathway not only failed to compensate for HR defects in these double mutant MEFs, but also was significantly impaired in these cells compared

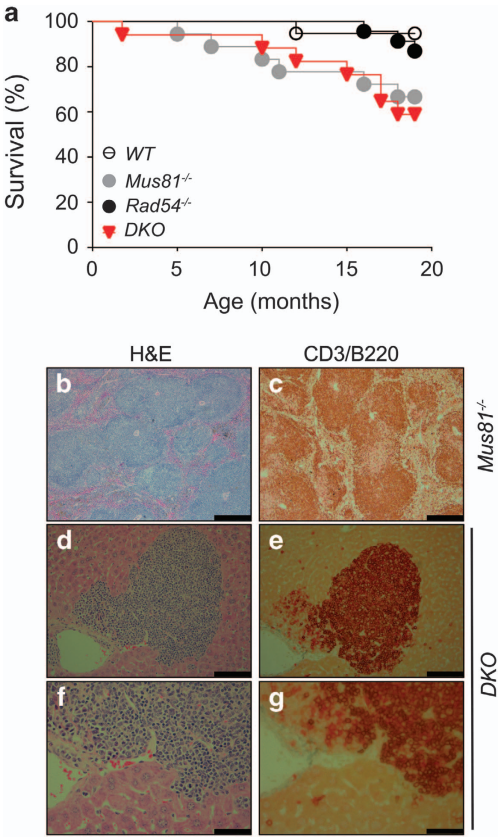

Figure 4. Rad54$^{-/-}$Mus81$^{-/-}$ mice and Mus81$^{-/-}$ controls display a similar risk of tumorigenesis. (**a**) Kaplan–Meier analysis representing the percent survival of cohorts of *WT* ($n=19$), *Rad54*$^{-/-}$ ($n=23$), *Mus81*$^{-/-}$ ($n=18$) and *Rad54*$^{-/-}$*Mus81*$^{-/-}$ (DKO; $n=16$) mice. (**b**–**g**) Representative images of staining with hematoxylin and eosin (H&E) (**b**, **d**, **f**) and anti-CD3/anti-B220 (**c, e, g**) of tumors from the indicated genotypes. H&E staining of lymphomas developed by *Mus81*$^{-/-}$ mice (**b**) and *Rad54*$^{-/-}$*Mus81*$^{-/-}$ mice (**d**, **f**). The DKO lymphomas invaded the liver (**d, f**). Staining with anti-B220 (brown) and anti-CD3 (purple) antibodies showed that these tumors were B220^{+} B-cell lymphomas (**c, e, g**). Scale bars: 100 μm (**b**–**e**); 50 μm (**f, g**).

with single mutant controls. This finding raises the possibility that, in addition to HR, Rad54 and Mus81 functions are required for efficient NHEJ-mediated repair; however, further studies are needed to identify the mechanisms by which loss of these two proteins affects the NHEJ repair pathway.

Our work demonstrates that despite their impaired HR and NHEJ-mediated repair and elevated levels of spontaneous DSBs, *Rad54*$^{-/-}$*Mus81*$^{-/-}$ mice show no increased tumor predisposition compared with *Mus81*$^{-/-}$ mice. One possibility for this apparently contradictory outcome is that elevated level of DNA damage in *Rad54*$^{-/-}$*Mus81*$^{-/-}$ primary cells leads to cytotoxicity, thereby preventing enhanced tumor incidence in double mutant mice compared with *Mus81*$^{-/-}$ littermates. Consistent with this possibility, spontaneous cell death was elevated in *Rad54*$^{-/-}$*Mus81*$^{-/-}$ mice compared with *Mus81*$^{-/-}$ littermates.

Consistent with the finding that the human endonuclease Mus81-Eme1 cleaves CFS and allows sister chromatid disjunction,[37,38] we observed reduced levels in fragile site breakage in *Mus81*$^{-/-}$ B cells compared with *WT* controls. Unexpectedly, our study also reveals an important role for Rad54 in replicative stress-inducible fragile site breakage.

Given that deficiency of MUS81 in human cells impairs cleavage of CFS and induces chromosomal segregation defects and mitotic failure,[37–40] it is possible that impaired cleavage of CFS in the absence of Rad54 and Mus81 contributes to the chromosomal missegregation and mitotic failure displayed by *Rad54*$^{-/-}$*Mus81*$^{-/-}$ cells. These defects, together with the elevated spontaneous DSBs in *Rad54*$^{-/-}$*Mus81*$^{-/-}$ primary cells, may trigger the death of these cells and as such serve a tumor-suppressor mechanism to prevent further increase of tumorigenesis risk in *Rad54*$^{-/-}$*Mus81*$^{-/-}$ mice compared with their *Mus81*$^{-/-}$ littermates.

Collectively, our data provide the first evidence for synergistic effects of Rad54 and Mus81 on DSB repair pathways *in vivo* and their role in chromosomal segregation and preventing mitotic defects. Although the loss of Rad54 in *Mus81*$^{-/-}$ mice resulted in impaired fertility, it did not further increase cancer risk in these mice, suggesting that defective cooperation of Rad54 and Mus81 can lead to different outcomes depending on the affected tissues and cells.

MATERIALS AND METHODS

Mice

Mus81$^{-/-}$ mice[14] were crossed with *Rad54*$^{-/-}$ mice[5] and double heterozygote mice were then crossed to obtain *Rad54*$^{-/-}$ *Mus81*$^{-/-}$ mice in a mixed 129/J x C57BL/6 genetic background. Mice were genotyped by PCR. All experiments were performed in agreement with the guidelines of the animal care committee of the Princess Margaret Cancer Centre. All mice used in the experiments were age matched.

In vivo sensitivity to IR and ICLs

Mice were treated with 8 Gy of IR or were intraperitoneally injected with 10 mg MMC/kg of body mass. At least seven mice per genotype were monitored for 30 days after the treatment. Mice were killed when they started loosing weight and became hunched and dehydrated or moribund. The day of killing was counted as the day of death.

Bone marrow colony-forming assay

Bone marrow cells from femurs of 8- to 10-week-old mice were seeded on 35 mm culture dishes (1×10^5 cells/ml in Methocult GF M3434 media—Stemcell Technologies Inc., Vancouver, BC, Canada). Cells were left untreated or irradiated and colonies were cultured for 10 days before counting.

Clonogenic assays

SV40-immortalized MEFs were seeded at 1000 cells per 60 mm dish and were either left untreated or treated with IR, MMC or PARPi. Ten days later, colonies were fixed with ice-cold methanol and stained with 25% methanol/crystal violet and were counted.

Analysis of chromosomal aberrations

Splenocytes from mice of 8- to 10 weeks of age were cultured (RPMI media, 10 μg/ml lipopolysaccharide, 10% fetal bovine serum) for 48 h in the presence MMC (40 ng/ml) or post-IR (2 Gy). Cells were blocked in mitosis using colcemid (0.1 μg/ml, 2 h), harvested, treated with hypotonic buffer (0.075 M KCl, 37 °C, 15 min), fixed (methanol 3:1 acetic acid, – 20 °C) and dropped on glass slides. Slides were stained for 10 min with 0.5 mg/ml of 4',6-diamidino-2-phenylindole (DAPI; Invitrogen, Carlsbad, CA, USA) and chromosome number and gross chromosomal aberrations were determined. Experiments were performed in triplicate and at least 40 metaphase spreads were analyzed per mouse per genotype. Slides were observed under a DMIRB epifluorescence microscope (Leica, Buffalo Grave, IL, USA) and images were acquired using a digital camera DC 300RF (Leica) and Leica Image Manager Software.

Immunofluorescence

SV40-immortalized MEFs were left untreated or irradiated with 5 Gy of IR. At different time points post-irradiation, cells were fixed (2% paraformaldehyde; 10 min) and incubated overnight with the following antibodies in dilution buffer (5% fetal bovine serum, 3% bovine serum albumin, 0.05% Triton X-100 in phosphate-buffered saline): anti-γ-H2ax (07-164, Millipore, Etobicoke, ON, Canada; 1:500 dilution), anti-53bp1 (A300-272A, Bethyl, Whistler, BC, Canada; 1:1000 dilution) or anti-Rad51 H92 (sc-8349, Santa Cruz Biotechnology, Dallas, TX, USA; 1:50 dilution). Cells were then incubated with a

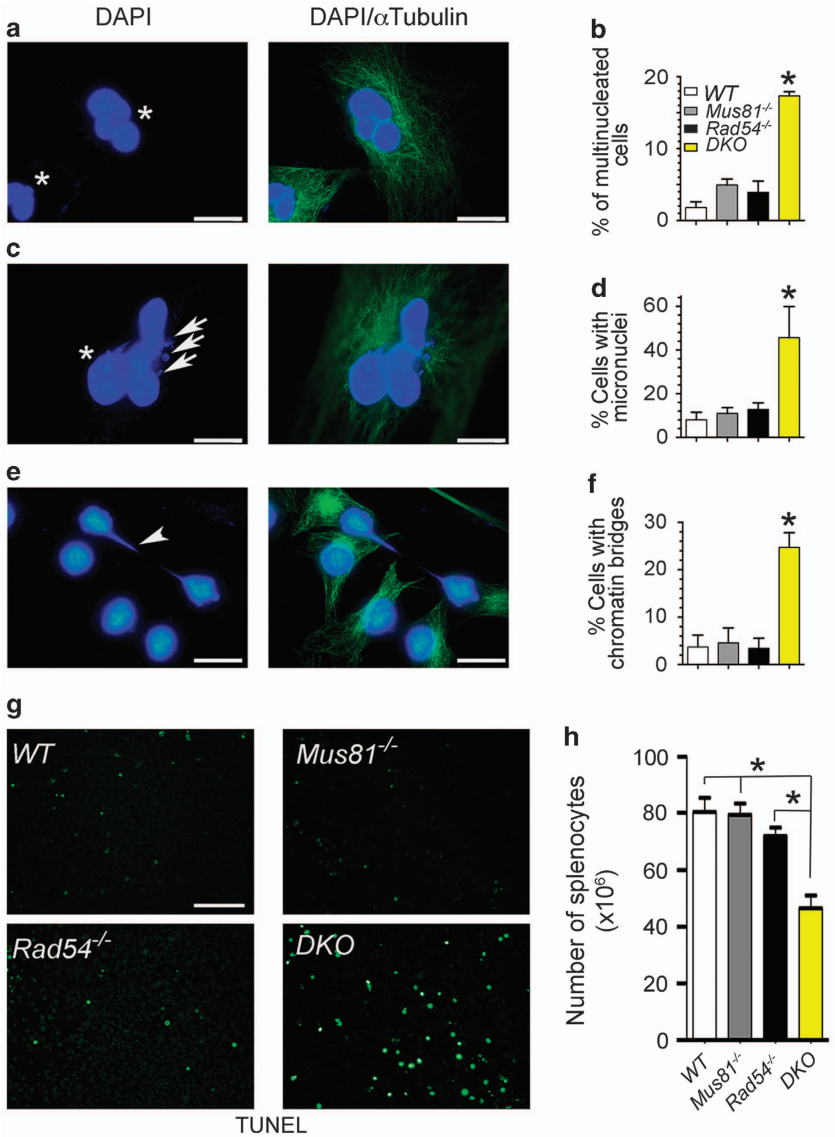

Figure 5. *Rad54*$^{-/-}$*Mus81*$^{-/-}$ cells display chromosomal segregation defects, impaired cleavage of CFSs and increased spontaneous death. (**a, c, e**) Representative images of abnormal *Rad54*$^{-/-}$*Mus81*$^{-/-}$ (DKO) MEFs showing multinuclei (**a**, **c**; asterisks), micronuclei (**c**, arrows) and chromatin bridges (**e**; arrow head). (**b**) Percentage of multinucleated cells in untreated SV40-immortalized *Rad54*$^{-/-}$*Mus81*$^{-/-}$ MEFs and controls. *$P < 0.0002$ compared with single mutant and *WT* controls. (**d**) Percentage of SV40-immortalized *Rad54*$^{-/-}$*Mus81*$^{-/-}$ MEFs and controls displaying micronuclei. *$P < 0.02$ compared with single mutant and *WT* MEFs. (**f**) Percentage of SV40-immortalized *Rad54*$^{-/-}$*Mus81*$^{-/-}$ MEFs and controls displaying chromatin bridges. *$P < 0.02$ compared with single mutant and *WT* MEFs. (**g**) Representative pictures of TUNEL staining performed on sections of spleens from 12-month-old *Rad54*$^{-/-}$*Mus81*$^{-/-}$ (DKO) mice and their *Rad54*$^{-/-}$, *Mus81*$^{-/-}$ and *WT* littermate controls. (**h**) Graph representing number of splenocytes from 12- to 13-month-old *Mus81*$^{-/-}$*Rad54*$^{-/-}$ mice and their single mutant and *WT* littermates. At least three independent experiments were performed. *$P < 0.001$. Bars: 20 μm (**a**, **c**), 50 μm (**e**) and 100 μm (**g**). All statistical analysis was performed using a two-tailed Student's *t*-test.

Table 2. Quantification of fragile site breakage in *Rad54*$^{-/-}$*Mus81*$^{-/-}$ B cells and their controls

B cells	*Total number of chromosomes*	*Total number of breaks*	*Breaks per chromosome*
WT (UT)	1552	30	0.019329897
WT (APH)	1428	68	0.047619048
Mus81$^{-/-}$ (UT)	1564	44	0.028132992
Mus81$^{-/-}$ (APH)	1103	44	0.039891206
Rad54$^{-/-}$ (UT)	1274	39	0.030612245
Rad54$^{-/-}$ (APH)	1007	26	0.025819265
Rad54$^{-/-}$*Mus81*$^{-/-}$ (UT)	1059	28	0.026440038
Rad54$^{-/-}$*Mus81*$^{-/-}$ (APH)	1119	36	0.032171582

Abbreviations: APH, aphidicolin; UT, untreated; WT, wild type. The number of chromosomes scored, breaks and breaks per chromosome are indicated for APH (0.2 μM) treated cells and their UT controls.

goat anti-rabbit Alexa fluor 488-conjugated antibody (A11008, Molecular Probes, Burlington, ON, Canada; 1:1000 dilution). Staining of untreated MEFs with anti-α-tubilin fluorescein isothiocyanate-conjugated monoclonal antibody (F-2168, Sigma, Markham, ON, Canada; 10:1000 dilution) was also performed. Next, cells were stained with DAPI and mounted on slides using Mowiol (Sigma). Stained cells were visualized and their foci quantified using a Leica DM 4000 B microscope. Image acquisition was performed using the Leica Application Suite V 4.0 software (Leica).

HR and NHEJ reporter assays

HR and NHEJ reporter constructs[36] were digested with I-*Sce*I restriction enzyme, and the linearized constructs, together with an red fluorescent protein (RFP) plasmid (internal control), were transfected into SV40-immortalized MEFs using a GenJet system (Frogga-Bio, North York, ON, Canada). Transfected cells were examined 48 h later by flow cytometry for their expression of green fluorescent protein (GFP) and RFP. Repair efficiencies of HR and NHEJ were expressed as GFP^+/RFP^+ ratios.

Immunoblotting

SV40-immortalized MEFs were harvested and lysed with HEPES buffer. In all, 100 μg of protein lysates were resolved by sodium dodecyl sulfate–polyacrylamide gel electrophoresis and probed with the following antibodies: anti-Brca1 (1:500; homemade), anti-53bp1 (1:2000; A300-272A, Bethyl), anti-Rad51 (1:2000; sc-8349, Santa Cruz Biotechnology) and anti-β-actin (Santa Cruz Biotechnology).

Fragile site assay

Metaphase chromosomes from B cells treated with 0.2 μM aphidicolin (Sigma) were dropped onto pre-hydrated glass slides (ThermoScientific, Burlington, ON, Canada) and aged at room temperature for 2–3 days. Chromosomes were then stained using Vectashield Mounting Medium containing DAPI (VWR, Mississauga, ON, Canada), and fragile site breakage was scored using a Zeiss LSM 700 light microscope (Birkerød, Danmark) equipped with Zen 2010 software (Birkerød, Danmark).

Histology

Paraffin sections of tumor and normal tissue were stained with hematoxylin and eosin, or exposed to anti-CD3 and anti-B220 antibodies to perform histological analysis as described in McPherson *et al.*[14] TUNEL staining was performed using a fluorescein *in situ* cell death detection kit as per the manufacturer's instructions (Roche Life Science, Laval, QC, Canada).

Statistical analysis

The following tests were used for statistical analysis: a paired *t*-test for comparisons among means, a log-rank (Mantel–Cox) test for comparisons among survival curves, and a two-sided Fisher's exact test using the Mstat software (Michigan, MI, USA) for comparison of the frequency of chromosomal aberrations and fragile site breakages. *P*-values below 0.05 were considered significant. The estimate of variation used is 95%.

CONFLICT OF INTEREST

The authors declare no conflict of interest.

ACKNOWLEDGEMENTS

This work was supported by the Canadian Institute of Health Research (RH). We thank P McPherson and members of the RH laboratory for helpful discussions and critical reading of the manuscript. In addition, we thank S Hakem for editing the manuscript and R Kanaar for providing *Rad54*$^{-/-}$ mice.

REFERENCES

1 Ciccia A, Elledge SJ. The DNA damage response: making it safe to play with knives. *Mol Cell* 2010; **40**: 179–204.
2 Prakash R, Zhang Y, Feng W, Jasin M. Homologous recombination and human health: the roles of BRCA1, BRCA2, and associated proteins. *Cold Spring Harb Perspect Biol* 2015; **7**: 4.
3 Mazin AV, Mazina OM, Bugreev DV, Rossi MJ. Rad54, the motor of homologous recombination. *DNA Repair (Amst)* 2010; **9**: 286–302.
4 Ceballos SJ, Heyer WD. Functions of the Snf2/Swi2 family Rad54 motor protein in homologous recombination. *Biochim Biophys Acta* 2011; **1809**: 509–523.
5 Essers J, Hendriks RW, Swagemakers SM, Troelstra C, de Wit J, Bootsma D *et al.* Disruption of mouse RAD54 reduces ionizing radiation resistance and homologous recombination. *Cell* 1997; **89**: 195–204.
6 Dronkert ML, Beverloo HB, Johnson RD, Hoeijmakers JH, Jasin M, Kanaar R. Mouse RAD54 affects DNA double-strand break repair and sister chromatid exchange. *Mol Cell Biol* 2000; **20**: 3147–3156.
7 Agarwal S, van Cappellen WA, Guenole A, Eppink B, Linsen SE, Meijering E *et al.* ATP-dependent and independent functions of Rad54 in genome maintenance. *J Cell Biol* 2011; **192**: 735–750.
8 Wesoly J, Agarwal S, Sigurdsson S, Bussen W, Van Komen S, Qin J *et al.* Differential contributions of mammalian Rad54 paralogs to recombination, DNA damage repair, and meiosis. *Mol Cell Biol* 2006; **26**: 976–989.
9 Essers J, van Steeg H, de Wit J, Swagemakers SM, Vermeij M, Hoeijmakers JH *et al.* Homologous and non-homologous recombination differentially affect DNA damage repair in mice. *EMBO J* 2000; **19**: 1703–1710.
10 Matsuda M, Miyagawa K, Takahashi M, Fukuda T, Kataoka T, Asahara T *et al.* Mutations in the RAD54 recombination gene in primary cancers. *Oncogene* 1999; **18**: 3427–3430.
11 Hussain SA, Palmer DH, Moon S, Rea DW. Endocrine therapy and other targeted therapies for metastatic breast cancer. *Expert Rev Anticancer Ther* 2004; **4**: 1179–1195.
12 Mazina OM, Mazin AV. Human Rad54 protein stimulates human Mus81-Eme1 endonuclease. *Proc Natl Acad Sci USA* 2008; **105**: 18249–18254.
13 Sarbajna S, West SC. Holliday junction processing enzymes as guardians of genome stability. *Trends Biochem Sci* 2014; **39**: 409–419.
14 McPherson JP, Lemmers B, Chahwan R, Pamidi A, Migon E, Matysiak-Zablocki E *et al.* Involvement of mammalian Mus81 in genome integrity and tumor suppression. *Science* 2004; **304**: 1822–1826.
15 Pamidi A, Cardoso R, Hakem A, Matysiak-Zablocki E, Poonepalli A, Tamblyn L *et al.* Functional interplay of p53 and Mus81 in DNA damage responses and cancer. *Cancer Res* 2007; **67**: 8527–8535.
16 Dendouga N, Gao H, Moechars D, Janicot M, Vialard J, McGowan CH. Disruption of murine Mus81 increases genomic instability and DNA damage sensitivity but does not promote tumorigenesis. *Mol Cell Biol* 2005; **25**: 7569–7579.
17 Hiyama T, Katsura M, Yoshihara T, Ishida M, Kinomura A, Tonda T *et al.* Haploinsufficiency of the Mus81-Eme1 endonuclease activates the intra-S-phase and G2/M checkpoints and promotes rereplication in human cells. *Nucleic Acids Res* 2006; **34**: 880–892.
18 El Ghamrasni S, Pamidi A, Halaby MJ, Bohgaki M, Cardoso R, Li L *et al.* Inactivation of chk2 and mus81 leads to impaired lymphocytes development, reduced genomic instability, and suppression of cancer. *PLoS Genet* 2011; **7**: e1001385.
19 Wechsler T, Newman S, West SC. Aberrant chromosome morphology in human cells defective for Holliday junction resolution. *Nature* 2011; **471**: 642–646.
20 El Ghamrasni S, Cardoso R, Halaby MJ, Zeegers D, Harding S, Kumareswaran R *et al.* Cooperation of Blm and Mus81 in development, fertility, genomic integrity and cancer suppression. *Oncogene* 2015; **34**: 1780–1789.
21 Wu F, Liu SY, Tao YM, Ou DP, Fang F, Yang LY. Decreased expression of methyl methansulfonate and ultraviolet-sensitive gene clone 81 (Mus81) is correlated with a poor prognosis in patients with hepatocellular carcinoma. *Cancer* 2008; **112**: 2002–2010.
22 Wu F, Shirahata A, Sakuraba K, Kitamura Y, Goto T, Saito M *et al.* Down-regulation of Mus81 as a potential marker for the malignancy of gastric cancer. *Anticancer Res* 2010; **30**: 5011–5014.
23 Wu F, Shirahata A, Sakuraba K, Kitamura Y, Goto T, Saito M *et al.* Downregulation of Mus81 as a novel prognostic biomarker for patients with colorectal carcinoma. *Cancer Sci* 2011; **102**: 472–477.
24 McPherson JP, Tamblyn L, Elia A, Migon E, Shehabeldin A, Matysiak-Zablocki E *et al.* Lats2/Kpm is required for embryonic development, proliferation control and genomic integrity. *EMBO J* 2004; **23**: 3677–3688.
25 Chu WK, Hickson ID. RecQ helicases: multifunctional genome caretakers. *Nat Rev Cancer* 2009; **9**: 644–654.
26 Zhu JY, Abate M, Rice PW, Cole CN. The ability of simian virus 40 large T antigen to immortalize primary mouse embryo fibroblasts cosegregates with its ability to bind to p53. *J Virol* 1991; **65**: 6872–6880.
27 Jackson SP, Bartek J. The DNA-damage response in human biology and disease. *Nature* 2009; **461**: 1071–1078.
28 Hakem R. DNA-damage repair; the good, the bad, and the ugly. *EMBO J* 2008; **27**: 589–605.

29 Boddy MN, Lopez-Girona A, Shanahan P, Interthal H, Heyer WD, Russell P. Damage tolerance protein Mus81 associates with the FHA1 domain of checkpoint kinase Cds1. *Mol Cell Biol* 2000; **20**: 8758–8766.
30 Interthal H, Heyer WD. MUS81 encodes a novel helix-hairpin-helix protein involved in the response to UV- and methylation-induced DNA damage in *Saccharomyces cerevisiae*. *Mol Gen Genet* 2000; **263**: 812–827.
31 Hanada K, Budzowska M, Modesti M, Maas A, Wyman C, Essers J *et al.* The structure-specific endonuclease Mus81-Eme1 promotes conversion of interstrand DNA crosslinks into double-strands breaks. *EMBO J* 2006; **25**: 4921–4932.
32 McManus KJ, Barrett IJ, Nouhi Y, Hieter P. Specific synthetic lethal killing of RAD54B-deficient human colorectal cancer cells by FEN1 silencing. *Proc Natl Acad Sci USA* 2009; **106**: 3276–3281.
33 Ahuja D, Saenz-Robles MT, Pipas JM. SV40 large T antigen targets multiple cellular pathways to elicit cellular transformation. *Oncogene* 2005; **24**: 7729–7745.
34 Tan TL, Essers J, Citterio E, Swagemakers SM, de Wit J, Benson FE *et al.* Mouse Rad54 affects DNA conformation and DNA-damage-induced Rad51 foci formation. *Curr Biol* 1999; **9**: 325–328.
35 Helleday T. The underlying mechanism for the PARP and BRCA synthetic lethality: clearing up the misunderstandings. *Mol Oncol* 2011; **5**: 387–393.
36 Mao Z, Jiang Y, Liu X, Seluanov A, Gorbunova V. DNA repair by homologous recombination, but not by nonhomologous end joining, is elevated in breast cancer cells. *Neoplasia* 2009; **11**: 683–691.
37 Ying S, Minocherhomji S, Chan KL, Palmai-Pallag T, Chu WK, Wass T *et al.* MUS81 promotes common fragile site expression. *Nat Cell Biol* 2013; **15**: 1001–1007.
38 Naim V, Wilhelm T, Debatisse M, Rosselli F. ERCC1 and MUS81-EME1 promote sister chromatid separation by processing late replication intermediates at common fragile sites during mitosis. *Nat Cell Biol* 2013; **15**: 1008–1015.
39 Garner E, Kim Y, Lach FP, Kottemann MC, Smogorzewska A. Human GEN1 and the SLX4-associated nucleases MUS81 and SLX1 are essential for the resolution of replication-induced Holliday junctions. *Cell Rep* 2013; **5**: 207–215.
40 Pepe A, West SC. MUS81-EME2 promotes replication fork restart. *Cell Rep* 2014; **7**: 1048–1055.
41 Durkin SG, Glover TW. Chromosome fragile sites. *Annu Rev Genet* 2007; **41**: 169–192.
42 Ozeri-Galai E, Bester AC, Kerem B. The complex basis underlying common fragile site instability in cancer. *Trends Genet* 2012; **28**: 295–302.
43 Heyer WD, Li X, Rolfsmeier M, Zhang XP. Rad54: the Swiss Army knife of homologous recombination? *Nucleic Acids Res* 2006; **34**: 4115–4125.
44 Sandra Muñoz-Galván CT, Blanco MG, Schwartz EK, Ehmsen KT, West SC, Heyer W-D *et al.* Distinct roles of Mus81, Yen1, Slx1-Slx4, and Rad1 nucleases in the repair of replication-born double-strand breaks by sister chromatid exchange. *Mol Cell Biol* 2012; **32**: 1592–1603.

Supplementary Information accompanies this paper on the Oncogene website (http://www.nature.com/onc)